Cell Reports, Volume *15*

Supplemental Information

Targeting Metabolic Symbiosis to Overcome Resistance to Anti-angiogenic Therapy

Laura Pisarsky, Ruben Bill, Ernesta Fagiani, Sarah Dimeloe, Ryan William Goosen, Jörg Hagmann, Christoph Hess, and Gerhard Christofori

Supplemental Information

Supplemental Figures

Figure S1. Related to Figure 1. Nintedanib treatment of Py2T cells *in vitro.*
(A) The inhibitory effect of increasing concentrations of nintedanib after 72 hours of treatment on Py2T tumor cell numbers has been determined by using an MTT assay *in vitro*. Data are shown as mean cell number normalized to control cells ± SD from three independent experiments.
(B) Representative immunofluorescence microphograph showing CD31-positive blood vessels in a tumor with a volume of 15mm^3 representing the time point at which treatments were generally initiated. DAPI was used to visualize cell nuclei. Scale bar, 50 µm.

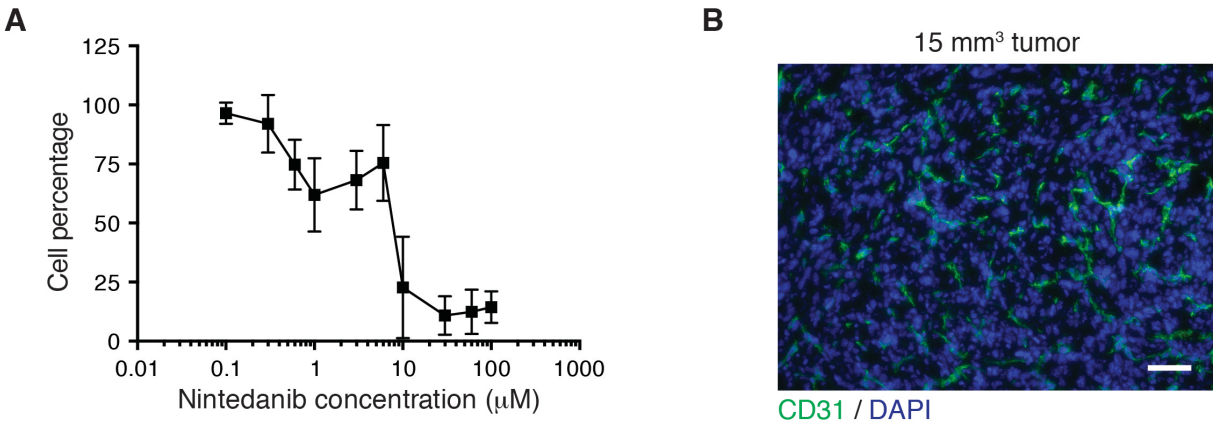

Figure S2. Related to Figure 2. Nintedanib and sunitinib treatments demonstrate potent anti-angiogenic effects.
(A) Representative images of immunofluoresecence stainings of tumor sections from ST and LT vehicle or nintedanib-treated mice with antibodies against CD31 are shown (C; green). DAPI was used to visualize cell nuclei. Scale bars, 50µm.
(B-D) Py2T tumor-bearing mice were treated with nintendanib or sunitinib during 21 days, and mice were sacrificed at day 35 post tumor cell injection. Tumor weights at the experimental end point (A), microvessel densities (B) and CD31-positive area fractions per field of view (C) determined by immunofluorescence staining are shown. N = 3-6 mice per group. Statistical significance was calculated using Mann–Whitney U test. n.s., non significant; *, $P < 0.05$; **, $P < 0.01$; ***, $P < 0.001$; ****, $P < 0.0001$.
(E) Blood vessel (CD31, red) coverage by perivascular cells (NG2, green) is shown on representative immunofluorescence pictures of tumors from ST and LT vehicle or nintedanib-treated mice. DAPI staining visualizes cell nuclei. Scale bars, 100µm.
(F) Blood vessel (CD31, red) perfusion (lectin, green) is shown on representative immunofluorescence pictures of tumors from ST and LT vehicle or nintedanib-treated mice. DAPI was used to visualize cell nuclei. Scale bars, 100µm.

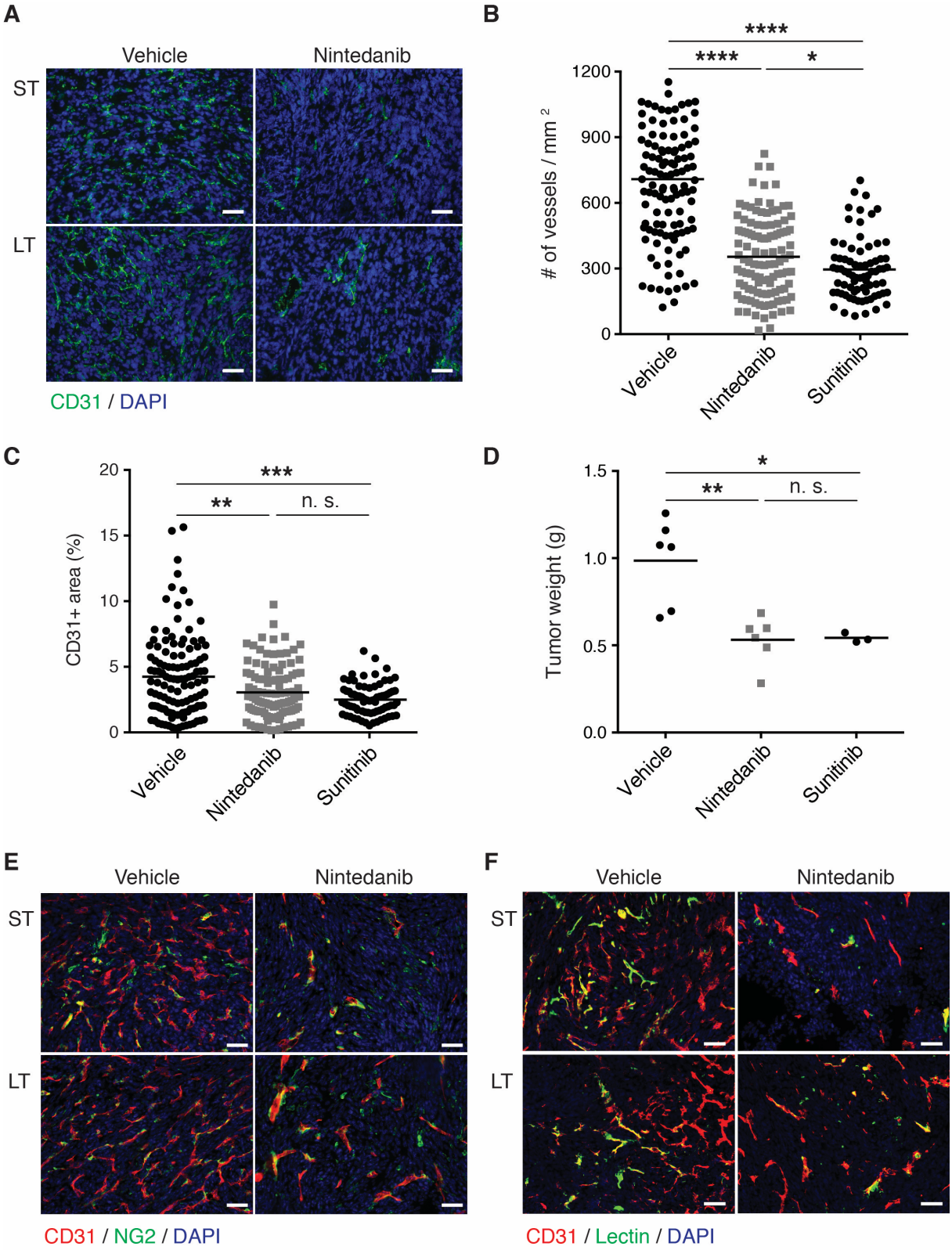
A
Vehicle
Nintedanib
ST
LT
CD31 / DAPI
B
****
****
*
1200
900
600
300
0
# of vessels / mm 2
Vehicle
Nintedanib
Sunitinib
C
***
**
n. s.
20
15
10
5
0
CD31+ area (%)
Vehicle
Nintedanib
Sunitinib
D
*
**
n. s.
1.5
1.0
0.5
0.0
Tumor weight (g)
Vehicle
Nintedanib
Sunitinib
E
Vehicle
Nintedanib
ST
LT
CD31 / NG2 / DAPI
F
Vehicle
Nintedanib
ST
LT
CD31 / Lectin / DAPI

Figure S3. Related to Figure 3. Flow cytometry cell sorting strategy.

(A) Representative flow cytometric analysis of a wild-type Py2T tumor confirming the absence of a CD8α-positive CD45-negative cell population. Relative frequencies of gated populations are shown.

(B) Schematic representation of the experimental setup. Py2T-CD8α cells were orthotopically injected into the mammary fat pad of FVB/N female mice. Two weeks later, after the angiogenic switch had occurred, nintedanib (50 mg/kg/day) treatment was initiated. One (ST) or three weeks (LT) after nintedanib initiation, corresponding ST and resistant LT-treated tumors, respectively, were harvested for cell isolation by flow cytometry.

(C) Schematic representation of the flow cytometry sorting strategy. Cells from dissociated tumors were separated by flow cytometry: tumor cells were identified by gating on the $CD45^-$ $CD8\alpha^+$ population, whereas endothelial cells were identified by gating on $CD45^-CD8\alpha^-$ $CD31^+podoplanin^-$ blood vessel endothelial cells.

(D) Representative results of cell sorting by flow cytometry. Cells were first gated for forward scatter (FSC) and sideward scatter (SSC), and propidium iodide-positive (PI) dead cells and cell doublets were excluded. Then, tumor cells were sorted by gating on the $CD45^-CD8\alpha^+$ population, whereas endothelial cells were sorted by gating on $CD45^-CD8\alpha^-$ $CD31^+podoplanin^-$ blood vessel endothelial cells.

(E) Expression of different glycolysis genes in Py2T cells cultured in hypoxic conditions analyzed by quantitative RT-PCR. Data are normalized to cells cultured in normoxic conditions. Shown are means ± SEM. N = 4. Statistical significance was calculated using Student t test. *, $P < 0.05$; **, $P < 0.01$; ***, $P < 0.001$; ****, $P < 0.0001$.

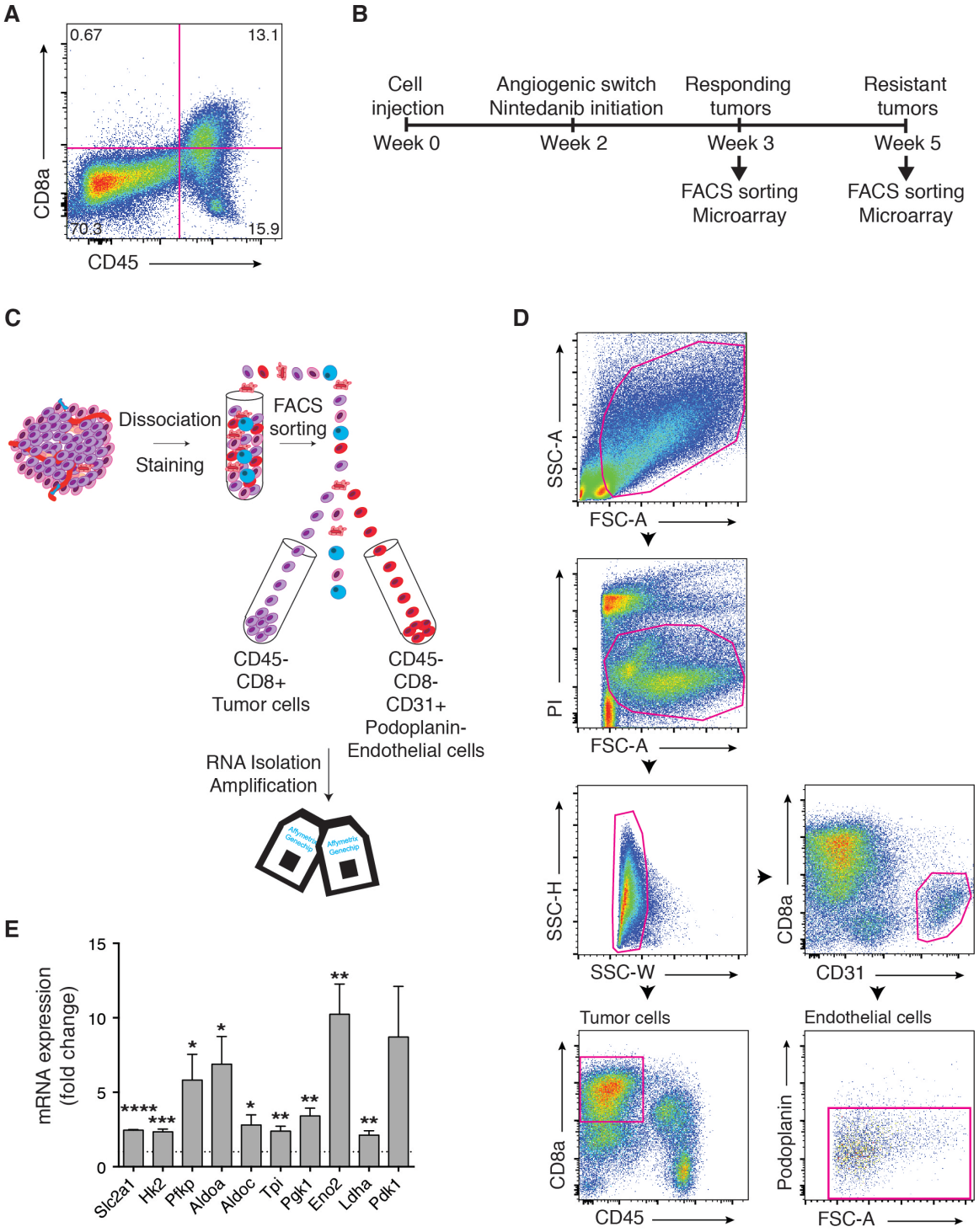
A
0.67
13.1
70.3
15.9
CD8a
CD45
B
Cell injection
Week 0
Angiogenic switch
Nintedanib initiation
Week 2
Responding tumors
Week 3
FACS sorting
Microarray
Resistant tumors
Week 5
FACS sorting
Microarray
C
Dissociation
Staining
FACS sorting
CD45-
CD8+
Tumor cells
CD45-
CD8-
CD31+
Podoplanin-
Endothelial cells
RNA Isolation
Amplification
D
SSC-A
FSC-A
PI
FSC-A
SSC-H
SSC-W
CD8a
CD31
Tumor cells
Endothelial cells
CD8a
CD45
Podoplanin
FSC-A
E
mRNA expression
(fold change)
15
10
5
0
****
***
*
*
*
**
**
**
**
Slc2a1
Hk2
Pfkp
Aldoa
Aldoc
Tpi
Pgk1
Eno2
Ldha
Pdk1

Figure S4. Related to Figure 4. Nintedanib treatment leads to the establishment of metabolic symbiosis.

(A) Lactate levels have been quantified in lysates of tumors from LT vehicle or nintedanib-treated mice, and are shown as mean ± SEM. N = 5 mice per group.

(B, C) Quantification of MCT1 (B) and MCT4 (C) expression by immunofluorescence staining on histological tumor sections from ST and LT vehicle or nintedanib-treated mice is shown. Mean MCT4 positive area fractions per each field of view are shown. N = 4 mice per group.

(D) Single channels corresponding to the MCT4/MCT1 co-staining presented in Figure 4A. Veh., vehicle; Nint., nintedanib. Scale bars, 100 μm.

(E) MCT4 expression in tumors derived from LT vehicle, nintedanib or sunitinib-treated mice was assessed by immunofluorescence staining. Values represent the MCT4-positive area fraction per each field of view. N = 5-6 mice per group.

(F, G) Shown are microvessel densities (F) and representative immunofluorescence stainings for MCT4 (G) in tumors of Rip1Tag2 transgenic mice treated for 3 weeks (LT) with nintedanib. DAPI was used to visualize cell nuclei. N = 8-9 mice per group. Scale bars, 100 μm.

(H-J) Single channels corresponding to MCT4/Glut1, pimonidazole/Glut1 and pimonidazole/MCT4 co-stainings presented in Figure 4E, 4G and 4I, respectively. Pimo., pimonidazole; Veh., vehicle; Nint., nintedanib. Scale bars, 100 μm.

(K) Mitochondrial biogenesis was identified and quantified by immunofluorescence staining for PGC1α in Py2T tumors from ST and LT vehicle or nintedanib-treated mice. N = 4 mice per group.

(L, M) Quantification of MCT4 expression in PGC1α+ area (L) by immunofluorescence staining on histological tumor sections from ST and LT vehicle or nintedanib-treated mice is shown together with some representative pictures (M). N = 4 mice per group. Scale bars, 50 μm.

(N) COX IV+ cell number was assessed by immunofluorescence staining on histological tumor sections from ST and LT vehicle or nintedanib-treated. N = 4 mice per group.

(O, P) Quantification of MCT4 expression in COX IV+ area (O) by immunofluorescence staining on histological tumor sections from ST and LT vehicle or nintedanib-treated mice is shown together with some representative pictures (P). N = 4 mice per group. Scale bars, 50 μm.

Statistical significance was calculated using Mann–Whitney U test. n.s., non significant; *, $P < 0.05$; **, $P < 0.01$; ***, $P < 0.001$; ****, $P < 0.0001$.

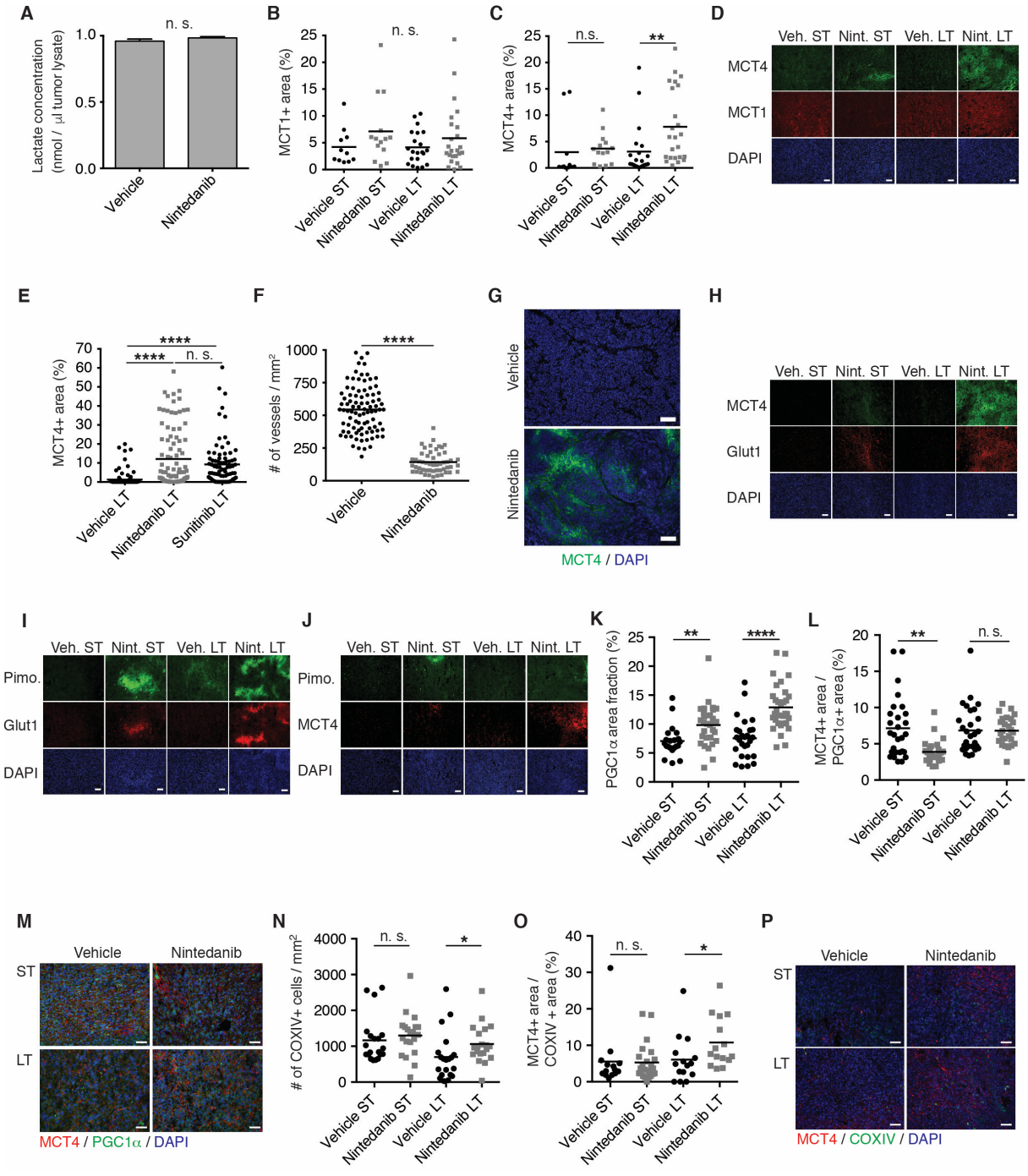
A
Lactate concentration (nmol / μl tumor lysate)
n. s.
Vehicle
Nintedanib
B
MCT1+ area (%)
n. s.
Vehicle ST
Nintedanib ST
Vehicle LT
Nintedanib LT
C
MCT4+ area (%)
n.s.
**
D
Veh. ST
Nint. ST
Veh. LT
Nint. LT
MCT4
MCT1
DAPI
E
MCT4+ area (%)
****
n. s.
Vehicle LT
Nintedanib LT
Sunitinib LT
F
# of vessels / mm2
Vehicle
Nintedanib
G
Vehicle
Nintedanib
MCT4 / DAPI
H
Glut1
I
Pimo.
J
K
PGC1α area fraction (%)
L
MCT4+ area / PGC1α+ area (%)
M
ST
LT
MCT4 / PGC1α / DAPI
N
# of COXIV+ cells / mm2
O
MCT4+ area / COXIV + area (%)
P
MCT4 / COXIV / DAPI

Figure S5. Related to Figure 5. Targeting glycolysis and metabolic symbiosis overcomes anti-angiogenic resistance.

(A, B) Primary tumor growth over time (A) and tumor weights at the experimental end point (B) of mice treated with either vehicle or nintedanib (50 mg/kg/day) in combination with 3PO (70 mg/kg/day) or solvent are shown. The mice were treated with 3PO 8 days after the initiation of nintedanib treatment and were analyzed 5 days later to determine early effects of 3PO therapy (short-term nintedanib and 3PO-treated mice). In (A), data are displayed as mean tumor volumes ± SEM.

(C) Hypoxic areas were identified and quantified by immunofluorescence staining for pimonidazole adducts in Py2T tumors treated as described in (A). Values represent the pimonidazole+ area fraction for each microscopic field of view and means are displayed.

(D, E) Quantification of total (D) and hypoxia- or normoxia-related (E) apoptosis by immunofluorescence co-staining for cCasp3 and pimonidazole in tumors from short-term nintedanib and 3PO-treated mice.

N = 4 mice per group.

(F) Representative western blot analysis of MCT4 expression in Py2T WT cells or Py2T CRISPR MCT4 Clones #1 and #2 cultured for 72h under normoxic or hypoxic condition.

(G) The efficiency of shRNA-mediated knockdown of MCT4 expression was determined by measuring the MCT4 mRNA levels of shCtrl or shMCT4 Py2T cells cultured in hypoxic or normoxic conditions by quantitative RT-PCR. Data are normalized to shCtrl Py2T cells cultured in normoxic conditions.

(H, I) Primary tumor growth (H) and terminal tumor weights (I) of mice following orthotopic injection of Py2T shCtrl or Py2T shMCT4 #2 and #5 cell lines treated with either vehicle or nintedanib (50 mg/kg/day) have been quantified. The time points for animal sacrifice were chosen for all three cell lines individually such that all the tumors of the corresponding vehicle-treated groups were size matched. In (B), mean ± SEM is depicted.

(J) Quantification of microvessel densities by immunofluorescence staining for CD31 on Py2T shMCT4 tumors from LT vehicle or nintedanib-treated mice. N = 6 mice per group.

(K) Quantification of MCT4 expression by immunofluorescence staining on histological sections from shCtrl or shMCT4 Py2T tumors treated either with nintedanib or vehicle is shown. Data displayed represents mean values per each field of view. N = 6 mice per group.

(L) MCT4 mRNA expression levels were analyzed by quantitative RT-PCR in shCtrl or shMCT4 Py2T tumors treated with either nintedanib or vehicle, and values are displayed as mean ± SEM. Data are normalized to shCtrl vehicle-treated tumors. N = 3 mice per group.

Statistical significance was calculated using Mann–Whitney *U* test. n. s., non significant; *, $P < 0.05$; **, $P < 0.01$; ****, $P < 0.0001$.

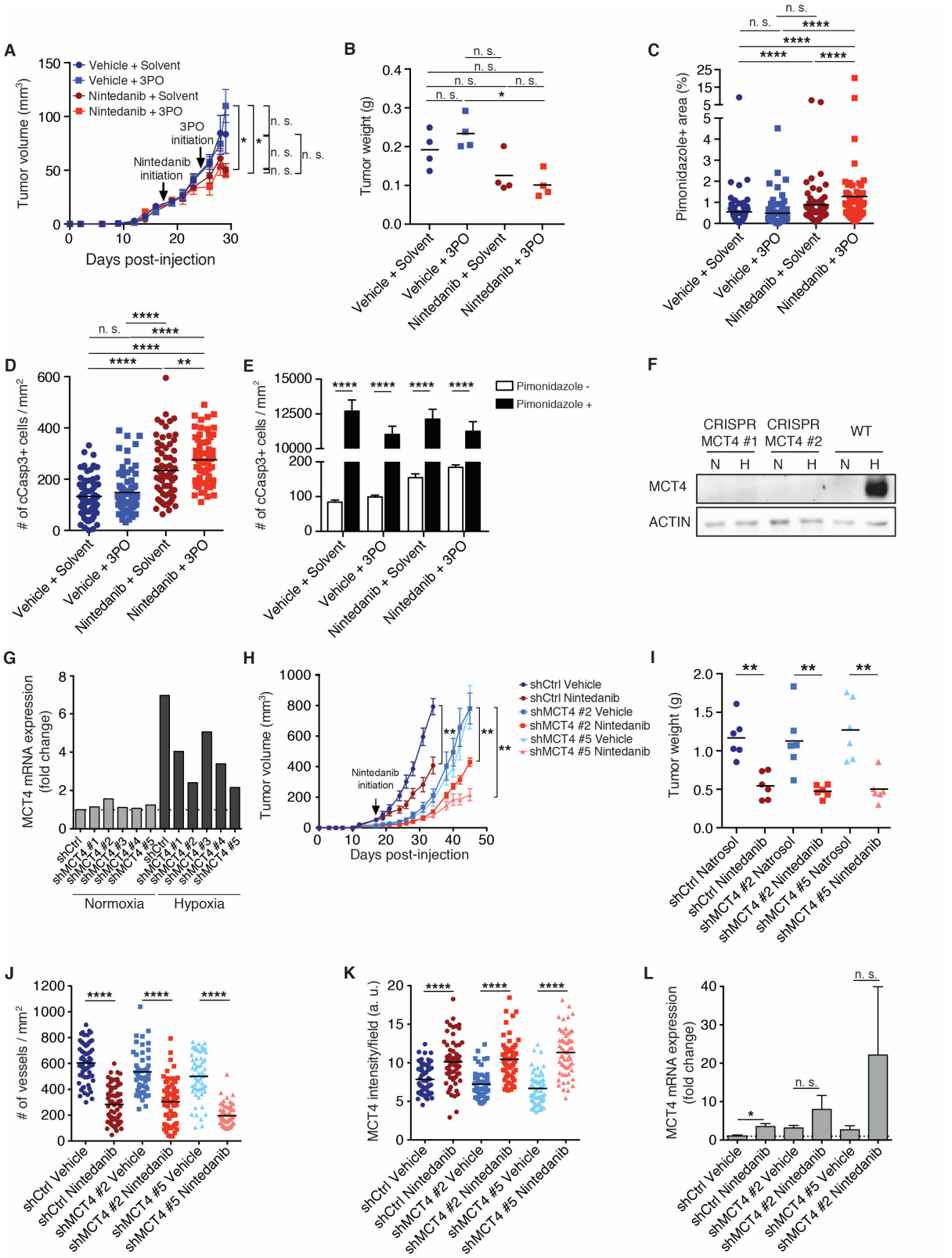
A
Vehicle + Solvent
Vehicle + 3PO
Nintedanib + Solvent
Nintedanib + 3PO
3PO initiation
Nintedanib initiation
Tumor volume (mm3)
Days post-injection
B
Tumor weight (g)
C
Pimonidazole+ area (%)
D
# of cCasp3+ cells / mm2
E
Pimonidazole -
Pimonidazole +
F
CRISPR MCT4 #1
CRISPR MCT4 #2
WT
MCT4
ACTIN
G
MCT4 mRNA expression (fold change)
Normoxia
Hypoxia
H
shCtrl Vehicle
shCtrl Nintedanib
shMCT4 #2 Vehicle
shMCT4 #2 Nintedanib
shMCT4 #5 Vehicle
shMCT4 #5 Nintedanib
I
J
# of vessels / mm2
K
MCT4 intensity/field (a. u.)
L
MCT4 mRNA expression (fold change)

Supplemental Experimental Procedures

Therapy studies

Treatment of Py2T tumor-bearing mice was initiated when tumors reached a measurable size (15-20mm^3) to allow a thorough stratification into experimental groups with similar mean tumor volumes. Nintedanib (kindly provided by Boehringer Ingelheim) was formulated in 0.5% natrosol hydroxyethylcellulose (Boehringer Ingelheim) and administered daily at 50 mg/kg body weight (BW) by oral gavage. Rip1Tag2 transgenic mice were treated with the same regimen from 10 weeks of age onwards (Bill et al., 2015). Sunitinib L-malate (LC Laboratories) was administered at 40 mg/kg in carboxymethylcellulose daily by oral gavage as described (Paez-Ribes et al., 2009). 3-(3-pyridinyl)-1-(4-pyridinyl)-2-propen-1-one (3PO; Axon Medchem, 2175) was dissolved in a 10% EtOH, 40% PEG, 50% PBS solution and administered at 70 mg/kg daily by intraperitoneal (i.p) injection. Treatment was initiated at day 8 of nintedanib treatment.

Animals of the experimental arms were euthanized by CO_2 (or cervical dislocation for hypoxia studies), either time- or size-matched to the control treatment. Primary tumors were dissected and processed for further analyses.

RNA isolation

RNA of sorted endothelial cells was isolated using the Absolutely RNA Nanoprep Kit (Stratagene) following the manufacturer's recommendations. RNA of sorted tumor cells was isolated using TRIzol® LS reagent (Ambion®) and RNA Easy Micro Kit (Qiagen). To isolate RNA from whole tumors, previously snap frozen tissues were homogenized in Tri Reagent (Sigma-Aldrich) using a POLYTRON® (Kinematica) and isolated following the manufacturer's recommendations.

Quantitative RT-PCR

RNA was reverse transcribed using M-MLV reverse transcriptase (Promega) and quantitative PCR was performed using SYBR-green PCR MasterMix (Applied Biosystems) in a StepOne Plus PCR machine (Applied Biosystems). Fold change expression was determined by the comparative Ct method ($\Delta\Delta C_t$) normalized to 60S Ribosomal protein L19 expression. Primers for quantitative PCR are listed in Table S1.

Lactate assay

Lactate concentration was determined on tumor lysate by using the L-Lactate Assay Kit from Abcam (ab65331) following the manufacturer's recommendations.

Immunoblotting

Immunoblotting has been performed as previously described (Zumsteg et al., 2012). The following antibodies were used: MCT4 (Santa Cruz Biotechnology, sc-50329, 1:200) and actin (Santa Cruz Biotechnology, sc-1616, 1:1000).

Lentiviral infection

Lentiviral plasmids containing short-hairpin RNAs #1-5 (shRNA) against mouse MCT4 were purchased from Sigma-Aldrich (Mission Non-Targeting shRNA control vector: SHC002; shMCT4 #1: TRCN0000079653, shMCT4 #2: TRCN0000079654, shMCT4 #3: TRCN0000079655, shMCT4 #4: TRCN0000079656, shMCT4 #5 TRCN0000079657). In order to produce lentiviral particles, HEK293T cells were transfected with the shRNA containing plasmids, the helper vectors pMDL and pREV and the envelope encoding plasmid pVSV using FugeneHD. Virus containing supernatant was conditioned for 2 days, filtered through a 0.45 µm filter, gently mixed with Lenti-X Concentrator (Clontech), and followed by an overnight incubation at 4°C and subsequent centrifugation the next day. The virus-containing pellet was resuspended in fresh complete DMEM medium, 8 ng/ml polybrene was added and Py2T cells were infected. Successfully transfected cells were selected by puromycin treatment (5 µg/ml). Knockdown efficiency was determined by measuring hypoxia-induced (96h, 1% O_2) MCT4 mRNA expression by quantitative RT-PCR.

Hypoxia and vessel functionality

To assess functional blood vessel perfusion, 100 µg of fluorescein-labeled Lycopersicon esculentum (tomato) lectin (Vector Laboratories, GL-1171) was injected into the tail vein. Two minutes later, mice were terminally anaesthetized and five minutes later perfused via the left cardiac ventricle first with cold 4% PFA and subsequently with cold PBS.

To identify hypoxic tumor areas, 60 mg/kg pimonidazole-HCl (Hypoxyprobe Omni Kits, Hypoxyprobe, Inc.) dissolved in PBS was injected i.p. 1 hour before euthanizing the animals by cervical dislocation.

Immunofluorescence microscopy analysis

Tumors were fixed in 4% PFA for 2 hours followed by overnight incubation in 20% sucrose to cryopreserve the tissue, both at 4°C. Then, tumors were snap frozen in Tissue-Tek OCT compound (Thermo Scientific) and stored at -80°C. Eight µm thick tumor sections were cut, dried for 30 minutes, rehydrated with PBS, permeabilized with 0.2% Triton X-100 for 20 minutes and blocked with 5% normal goat serum (NGS; Sigma-Aldrich) for 1 hour. As an exception, when performing stainings with anti-cCasp3 antibodies, blocking was performed using 20% NGS. When using a goat primary antibody, sections were blocked with 5% bovine serum albumin. Subsequently, primary and secondary antibodies were diluted in blocking solution and incubated overnight at 4°C and 1 hour at room temperature, respectively. Images were acquired with a Leica DMI 4000 microscope.

Antibodies used: rabbit anti-cleaved Caspase-3 (cCasp3; Cell Signaling, 9664, 1:50), rat anti-CD31 (BD Pharmingen, 550274, 1:50), rabbit anti-NG2 (Chemicon, AB5320, 1:100), rabbit anti-phospho Histone H3 (pH3; Millipore, 06-570, 1:200), rabbit anti-pimonidazole (Hypoxyprobe, 1:25), mouse anti-pimonidazole-FITC (Hypoxyprobe, 1:25), goat anti-MCT1 (Santa Cruz, sc-14917, 1:50), rabbit anti-MCT4 (Santa Cruz, sc-50329, 1:50), goat anti-MCT4 (Santa Cruz, sc-14930, 1:50), goat anti-Glut1 (Santa Cruz, sc-1605, 1:50), rabbit anti-CoxIV (Cell Signaling, 4850, 1:100) and rabbit anti-PGC1α (Millipore, AB3242, 1:300). Primary antibody binding was detected by incubating the histological sections with secondary antibodies directed against the respective species of the primary antibodies for 1 hour at room

temperature, diluted 1:200 in blocking solution. Secondary antibodies were fluorescently tagged with Alexa 488, Alexa 568 or Alexa 633 (Molecular probes). Subsequently, nuclei were stained with 4′,6-Diamidin-2-phenylindol (DAPI; Sigma-Aldrich; 1:10,000) followed by mounting the slides with Dako mounting medium (Dako).

Flow cytometry

Freshly dissected Py2T primary tumors were immediately minced into small pieces and digested for 30 minutes at 37°C on a bacterial shaker in DMEM (Sigma-Aldrich) supplemented with Nu-Serum Growth Medium Supplement (6%; Corning), DNase I (200 µg/ml; Roche), Dispase II (1.2mg/ml; Roche) and Collagenase D (1.2 mg/ml; Roche). To achieve a single cell suspension, the digested tissue was first passed through a 70 µm and subsequently through a 40 µm cell strainer (Corning). Cells were washed in FACS-buffer (5% fetal bovine serum in PBS; Sigma-Aldrich). Fc-receptors were blocked with an antibody against CD16/CD32 (BioLegend, 101302, 1:100) diluted in FACS-buffer for 30 minutes at 4°C. Then, cells were incubated for 45 minutes on ice with the following antibodies: hamster anti-mouse podoplanin (Hybridoma supernatant clone 8.1.1, 1:10), anti-CD8α-FITC (BioLegend, 100705, 1:150), anti-CD31-APC (BioLegend, 102409, 1:200), anti-CD45-APC-Cy7 (BioLegend, 103116, 1:500). Staining for podoplanin was achieved by subsequently incubating the cells for 30 minutes on ice with an anti-hamster PE-labeled secondary antibody (eBioscience, 12-4112-83, 1:200). Immediately before sorting with a FACSAriaII (BD Bioscience), cells were filtered through a 40 µm mesh and propidium iodide (PI) was added to exclude dead cells. Tumor cells were sorted into FACS-buffer by gating on $CD8\alpha^{+}/CD45^{-}$ cells (Figure S3D). Endothelial cells were directly sorted into the lysis buffer of the Absolutely RNA Nanoprep Kit (Stratagene) by gating on $CD31^{+}/CD45^{-}/Podoplanin^{-}$ cells (Figure S3D).

Annexin V staining

Py2T WT cells or Py2T CRISPR MCT4 clones #1 and #2 were cultured for 3 days under normoxic or hypoxic conditions. Both floating and attached cells were collected and washed in PBS. 1.10^{6} cells were resuspended in 1X binding buffer and stained using Cy5 AnnexinV (BD Pharmingen, # 559934, dilution 1/20) and 2 µg/ml DAPI for 20 min in the dark. 50,000 cells/sample were analyzed by flow cytometry (FACS Canto, Becton Dickinson).

EdU staining

Py2T WT cells or Py2T CRISPR MCT4 clones #1 and #2 were cultured for 3 days under normoxic or hypoxic conditions. Cells were incubated with 10 µM EdU for 30 min. After trypsinization 1.10^{6} cells were stained using EdU-Flow cytometry 488 Kit (Base-Click, BCK-FC488) following manufacturer's instruction. Prior to FACS acquisition cells were incubated 2h at 37°C in presence of 10 µg/ml RNAse (Roche, 11119915001) and 50 µg/ml propidium iodide (Sigma-Aldrich, 81845). 50,000 cells/sample were analyzed by flow cytometry (FACS Canto, Becton Dickinson).

Extracellular metabolic flux analysis

For analysis of the OCR (in pmol/min) and ECAR (in mpH/min), the Seahorse XFe-96 metabolic extracellular flux analyzer was used (Seahorse Bioscience, North Billerica, MA, USA). Py2T WT cells or Py2T CRISPR MCT4 clones #1 and #2 were plated at a density of 2,500 cells per well and expanded for 48 hours under normoxic (21% O_2) or hypoxic (1% O_2) conditions. Cells were treated with nintedanib for 48h or with 3PO for 3h. Prior to performing the metabolic assays, medium was exchanged for serum-free unbuffered RPMI-1640 medium (Sigma-Aldrich). Perturbation profiling of mitochondrial respiratory parameters was performed by the addition of oligomycin (1 μM), Carbonyl cyanide-4-(trifluoromethoxy)phenylhydrazone (FCCP) (2 μM) and rotenone (1 μM) and measuring changes in OCR. Glycolytic parameters were assessed independently in parallel wells by the sequential addition of glucose (10 mM), oligomycin (1 μM) and 2-deoxyglucose (2-DG, 50 mM, all Sigma-Aldrich) to cells maintained in glucose-free unbuffered RPMI-1640 medium (Sigma-Aldrich). Metabolic parameters were calculated following the manufacturer's recommandation. Additionally, OCR and ECAR were assessed under hypoxic conditions (1% O2) using the Seahorse XFe-96 metabolic extracellular flux analyzer placed in a Hypoxia Workstation (SCI-tive, Ruskinn Technology, Bridgend, UK). Unbuffered medium (± glucose) was equilibrated to hypoxia overnight and layered onto) Py2T WT cells or Py2T CRISPR MCT4 clones #1 and #2 plated as described above. Metabolic parameters were assessed as per under normoxic conditions and there were additional control wells where 1 M sodium sulfite was injected into calibrant fluid to provide a 'zero' oxygen reference parameter for the software algorithm to calculate OCR.
The different parameters have been calculated as follows: ATP-coupled respiration = [OCR(basal-non corrected basal OCR)] - [OCR(oligomycin)]; glycolysis = [ECAR(glucose)] – [ECAR(basal-non corrected basal ECAR)]; glycolytic capacity = [ECAR(oligomycin)] – [ECAR(basal-non corrected basal ECAR)]; glycolytic reserve = [ECAR(oligomycin)] – [ECAR(glucose)].

Microarray analysis
Total RNA preparations of flow cytometry-sorted tumor and endothelial cells were analyzed using an Agilent 2100 bioanalyzer. Target synthesis was performed using the following suite of kits provided by Nugen (San Carlos, USA): WT-Ovation Pico (Cat# 3300), WT-Ovation Exon (Cat# 2000) and FL-Ovation Biotin V2 (Cat# 4200). The hybridization cocktail (200µl) containing fragmented biotin-labeled target DNA at a final concentration of 25ng/µl was transferred into Affymetrix GeneChip MoGene-1_0-st-v1 (Affymetrix) and incubated at 45°C on a rotator in a hybridization oven 640 (Affymetrix) for 17 h at 60 rpm. The arrays were washed and stained on a Fluidics Station 450 (Affymetrix) by using the Hybridization Wash and Stain Kit (Affymetrix, Cat# 900720) and the Fluidics Procedure FS450_0001. The GeneChips were processed with an Affymetrix GeneChip® Scanner 3000 7G (Affymetrix). DAT image files of the microarrays were generated using Affymetrix GeneChip Command Console (AGCC, version 0.0.0.676, Affymetrix).

Bioinformatic analysis
All microarray data were preprocessed and analyzed using R (software environment for statistical computing and graphics) version 3.1.0 (2014-04-10) and packages provided by the

Bioconductor package library. Raw Affymetrix CEL files were subjected to background correction and normalization using the Robust Multichip Average (RMA) algorithm (rma method, oligo package). Differential gene expression was determined using the limma package (Smyth et al., 2005) with and without a p-value cutoff of 0.05 and a range of fold-change values (FC = 1.2 to 1.7). The results of differential gene expression were used to conduct pathway enrichment analysis provided by The Database for Annotation, Visualization and Integrated Discovery (DAVID) v6.7 (Huang da et al., 2009), with a particular focus on pathways defined in the Kyoto Encyclopedia of Genes and Genomes (KEGG) database.

The background-corrected and normalized gene expression datasets associated with the placebo-treated (UT), 1 week-treated (ST), and 3 week-treated (LT) samples were subjected to Gene Set Enrichment Analysis (GSEA) using GSEA V2.1.0. Three sets of analyses were conducted: ST *versus* UT, LT *versus* UT and ST *versus* LT. In all cases the default run-time arguments were used except for the "Permute" parameter that was set to "gene_set" (in order to accommodate less than 7 samples per class). In addition, analyses were conducted against the "MoGene_1_0_st.chip" microarray annotation and the following gene set libraries: "c2.cp.kegg.v4.0.symbols.gmt" and "c2.cp.reactome.v4.0.symbols.gmt" (Mootha et al., 2003; Subramanian et al., 2005).

Heat maps were generated using the heatmap.2 method provided by the gplots package. Boxplots were generated using the default boxplot method provided in R and based on the median background corrected and normalized expression value for each gene with respect to all samples within each sample class (UT, ST and LT). Additional statistical analyses were also carried out using GraphPad Prism 6 (GraphPad Prism Software Inc.).

The microarray data has been deposited on Gene Expression Omnibus platform under the accession number GSE78698.

Primers for qRT-PCR

Name	Sequence (5' - 3')
Glut1 (Slc2a1)	gaccctgcacctcattgg
	gatgctcagataggacatccaag
Hexokinase 2 (Hk2)	gctgaaggaagccattcg
	tcccaactgtgtcatttaccac
Phosphofructokinase, platelet (Pfkp)	gctatcggtgtcctgacca
	actttggcccccgtgtag
Aldolase A (Aldoa)	aaggaagaggttcctctaaagacc
	aatgcggtgagcgatgtc
Triosephosphate isomerase 1 (Tpi1)	ttcgagcaaaccaaggtcat
	ccggagcttctcgtgtactt
Phosphoglycerate kinase 1 (Pgk1)	gaagtcgagaatgcctgtgc
	ccggctcagctttaacctt
Enolase 2 (Eno2)	aacagcgttacttaggcaaagg
	ccaccacggagatacctgag
Lactate dehydrogenase A (Ldha)	ggcactgacgcagacaag
	tgatcacctcgtaggcactg
Pyruvate dehydrogenase kinase 1 (Pdk1)	gttgaaacgtcccgtgct
	gcgtgatatgggcaatcc
β-actin (Actb)	ctaaggccaaccgtgaaaag
	accagaggcatacagggaca
Peroxisome proliferator-activated receptor gamma coactivator 1 alpha (Pgc1a)	tgaggaccagcctctttgccca
	cgctacaccacttcaatccaccc
Cytochrome c oxidase subunit IV isoform 1 (Cox4i1)	tacttcggtgtgccttcga
	tgacatgggccacatcag
Monocarboxylate transporter 4 (Scl16a3)	gctcacctcctcccttgtg
	ctcttcctcttcccgatgc
60 ribosomal protein L19 (Rpl19)	ctcgttgccggaaaaaca
	tcatccaggtcaccttctca

Supplemental References

Mootha, V.K., Lindgren, C.M., Eriksson, K.F., Subramanian, A., Sihag, S., Lehar, J., Puigserver, P., Carlsson, E., Ridderstråle, M., Laurila, E., *et al.* (2003). PGC-1alpha-responsive genes involved in oxidative phosphorylation are coordinately downregulated in human diabetes. Nat Genet *34*, 267-273.

Smyth, G.K., Michaud, J., and Scott, H.S. (2005). Use of within-array replicate spots for assessing differential expression in microarray experiments. Bioinformatics *21*, 2067-2075.

Subramanian, A., Tamayo, P., Mootha, V. K., Mukherjee, S., Ebert, B. L., Gillette, M. A., Paulovich, A., Pomeroy, S. L., Golub, T. R., Lander, E. S., and Mesirov, J. P. (2005). Gene set enrichment analysis: a knowledge-based approach for interpreting genome-wide expression profiles. Proceedings of the National Academy of Sciences of the United States of America *102*, 15545-15550.

Sherman, B.T., Huang da, W., Tan, Q., Guo, Y., Bour, S., Liu, D., Stephens, R., Baseler, M.W., Lane, H.C., and Lempicki R,A. (2007). DAVID Knowledgebase: a gene-centered database integrating heterogeneous gene annotation resources to facilitate high-throughput gene functional analysis. BMC Bioinformatics *8*, 426.

Zumsteg, A., Caviezel, C., Pisarsky, L., Strittmatter, K., García-Echeverría, C., Hofmann, F., and Christofori, G. (2012). Repression of malignant tumor progression upon pharmacologic IGF1R blockade in a mouse model of insulinoma. Mol Cancer Res. *10*, 800-809.